UK Atomic Energy Authority

UKAEA-STEP-CP(23)02

J.H.P. Rice, J. Geng, C.W. Bumby, H.W. Weijers, S. Wray, H. Zhang, F. Schoofs, D. Moseley, R.A. Badcock

Design of a 60 kA Flux Pump for Fusion Toroidal Field Coils paper

Design of a 60 kA Flux Pump for Fusion Toroidal Field Coils paper

J.H.P. Rice, J. Geng, C.W. Bumby, H.W. Weijers, S. Wray, H. Zhang, F. Schoofs, D. Moseley, R.A. Badcock

This paper has been submitted to
15th European Conference on Applied Superconductivity (EUCAS), Virtual Conference, 5 September 2021

Design of a 60 kA Flux Pump for Fusion Toroidal Field Coils

James H.P. Rice, Jianzhao Geng, Chris W. Bumby, Hubertus W. Weijers *Senior Member, IEEE*, Dominic Moseley *Member, IEEE*, Steven Wray, Heng Zhang, Frank Schoofs and Rodney A. Badcock *Senior Member, IEEE*.

***Abstract*—High-Temperature Superconducting (HTS) magnets offer a novel pathway to magnetically confined fusion energy generation. Reactor-scale fusion devices require tens of kA of current to generate large toroidal fields for magnetic confinement. Operating HTS magnets at kA-current levels is difficult due to unavoidable joint resistances that require active driving of current. The large footprint and energy demand of a solid-state power supply and multi-kA current leads present significant constraints on the size, cost and efficiency of a fusion tokamak. An alternative approach is to use an HTS Flux Pump, which can generate and sustain persistent currents in HTS coils at the kA-levels required by fusion magnet systems. Here, we outline the design of a 60 kA transformer-rectifier flux pump for energizing and sustaining an 80 mH HTS fusion magnet. The flux pump is driven by an iron-core transformer with copper primary and HTS secondary windings. This is rectified by switching elements in the superconducting circuit into a dc voltage output which charges the inductive load. To charge the load coil to 60 kA in 24 hours, an output dc voltage of 55 mV is needed. However, only 6 mV is required to maintain a long-term steady current of 60 kA. Such a device can significantly reduce the cost and footprint of future fusion reactor designs.**

***Index Terms*—Tokamak, Fusion, HTS Flux Pump, efficiency, switch rectifier.**

I. Introduction

FUSION Energy research aims to produce a large amount of electrical power to national grids in a way that is safe, sustainable, and economic. A prominent method of magnetic confinement is the tokamak, which uses strong Toroidal Field (TF) coils to confine the fuel plasma. Generating the high fields necessary uses large, superconducting electromagnets [1], [2]. The ITER project [3] in France gives a good indication of a reactor-scale tokamak. ITER's magnet systems contain 18+1 Nb_3Sn TF coils, each carrying 68 kA to generate a toroidal field of 5.3 T, with a total stored energy of 41 GJ. This corresponds to an inductance of roughly 250 mH per magnet coil. Energizing and sustaining such an inductive load at high current is extraordinarily difficult, requiring large, reactive power-electronic systems [4]. Using conventional power systems requires conveying the current between room temperature and 4.5 K using current leads [5]. Current leads unavoidably leak heat into the cryostat; up to 100 WkA^{-1} for gas-cooled leads [6]. Any heat in the cryostat must be removed at the cryogenic cooling penalty, with cryogenic system making up 80% of the ITER power budget [7]. Moreover, significant additional voltage is dropped across resistive components, whose loss goes as I_2R, further increasing the required power input. Overall, these factors reduce the engineering power gain Q_E of the reactor, and negatively impact economic viability.

High-Temperature Superconducting (HTS) Flux Pumps are superconducting power supplies [8]–[18] that can energize high currents in inductive superconducting load coils. Load current outputs of >1 kA have been demonstrated in recent years [19]–[21]. Large load currents can then be sustained indefinitely in a quasi-Persistent Current Mode (qPCM) [22]. HTS Flux Pumps wirelessly generate voltage from within the cryostat itself [23], foregoing the need for current leads to room temperature. They are also characterized by significantly lower internal impedance than conventional supplies [24]. Utilizing flux pumps to energize tokamak TF coils may significantly reduce required input power, improving the overall power balance of tokamak reactors.

Transformer-rectifier flux pumps (TRFP) [13], [14], [17] act as ac current to dc voltage converters. Ac current is induced in a superconducting circuit and rectified into voltage across a load coil, using superconducting switching elements. The circuit can be arranged in half- or full-wave configurations, as shown in Fig. 1. Switching elements can employ either dynamic resistance from ac loss [13], [24] or non-linear flux flow resistance [14], [25] to generate useful voltage. In either case, the flux pump can be closely modelled using a simple circuit topology [26]. The transformer wirelessly transfers ac current from a room temperature primary to a superconducting secondary. The ac current waveform is shown in Fig. 1c). The load current is sustained between charging cycles through the parallel 'bridge' switch when in the 'closed' state of no resistance. To prevent the transformer from saturating [27], flux across the switches must be conserved within a cycle [21]

$$\frac{1}{T}\int_0^T v_1\,\mathrm{d}t = \frac{1}{T}\int_0^T v_2\,\mathrm{d}t \tag{1}$$

where $f = 1/T$ is the frequency of the input current, and v_1 and v_2 are the instantaneous voltages across the series and

This work was supported in part by the New Zealand Ministry of Business, Innovation and Employment (MBIE RTVU1916), and has been part-funded by STEP, a UKAEA programme to design and build a prototype fusion energy plant and a path to commercial fusion.

J. H.P. Rice, J. Geng, C. W. Bumby, H. W. Weijers, and R.A. Badcock are with the Robinson Research Institute, Victoria University of Wellington, Lower Hutt 5010, New Zealand. (e-mail: james.rice@vuw.ac.nz).

J. Geng is also with the Huazhong University of Science and Technology, Wuhan, Hubei, China.

S. Wray, H. Zhang and F. Schoofs are with the UK Atomic Energy Authority, Culham Science Centre, Abingdon OX14 3DB United Kingdom.

Manuscript received September 6th, 2021.

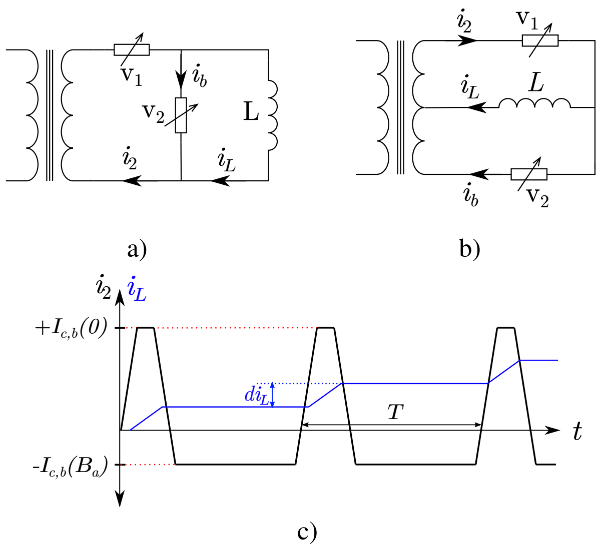

Fig. 1. Circuit diagrams of both a) half- and b) centre-tap full-wave TRFP. Switches are depicted as variable resistors, v_1 and v_2, and the load coil as the inductor L. The transformer is taken to have a resistive copper primary and superconducting secondary. c) Input trapezoidal waveform with transformer secondary current i_2 (black) and load current i_L (blue), with load current charging increment di_L.

parallel switches, respectively.

Until now, little attention has been given to the power efficiency of HTS flux pumps [25], [28]. Power transfer efficiency can be used to relate output power to the heat loss of switching, and therefore the losses in the cryostat. This makes it a useful tool in calculating the expected cryogenic heat load of a flux pump and is the focus of this work.

II. Ideal Flux Pump Efficiency

Beginning with the half-wave rectifier (Fig. 1a)), the efficiency η is the ratio of output power delivered to the load and total power dissipated in the circuit.

$$\eta = \frac{P_{\text{out}}}{P_{\text{out}} + P_{\text{sw}}} \tag{2}$$

where P_{out} is the output power to the load, and P_{sw} is the power dissipated in switching components. The cycle-average values of these components are

$$P_{\text{out}} = \frac{1}{T}\int_0^T v_2 \cdot i_L \,\mathrm{d}t, \tag{3}$$

$$P_{\text{sw}} = \frac{1}{T}\int_0^T (v_1 \cdot i_2 + v_2 \cdot i_b) \,\mathrm{d}t; \tag{4}$$

which leads to

$$\eta = \frac{\int_0^T i_L \cdot v_2 \,\mathrm{d}t}{\int_0^T i_L \cdot v_2 \,\mathrm{d}t + \int_0^T (v_1 \cdot i_2 + v_2 \cdot i_b) \,\mathrm{d}t} \tag{5}$$

where i_2, i_b, and i_L are the instantaneous transformer secondary, bridge, and load currents, respectively. Instantaneous values of current and voltage are distinguished from steady-state values by the use of lower case. Eq. 5 can be used to numerically calculate ideal efficiency each cycle.

Rectification occurs when the cycle-average of bridge voltage v_2 is non-zero, resulting in output voltage across the load. For sufficiently small injections of current in each cycle, for example at load saturation with low current ripple, $di_L \ll i_L$ and i_L can be removed from the integral as a constant.

$$\eta = \frac{i_L \int_0^T v_2 \,\mathrm{d}t}{i_L \int_0^T v_2 \,\mathrm{d}t + \int_0^T (v_1 \cdot i_2 + v_2 \cdot i_b) \,\mathrm{d}t} \tag{6}$$

Eq. (1) equates cycle-averaged switching voltages, giving

$$\eta = \frac{i_L \int_0^T v_2 \,\mathrm{d}t}{i_L \int_0^T v_2 \,\mathrm{d}t + 2\int_0^T v_2 \cdot (i_2 + i_b) \,\mathrm{d}t}. \tag{7}$$

Using a critical state model, voltage is generated when $i < I_c$. This limits instantaneous currents to critical currents when switched, allowing current to be removed as constant

$$\eta = \frac{i_L \int_0^T v_2 \,\mathrm{d}t}{i_L \int_0^T v_2 \,\mathrm{d}t + 2\,(I_{2-} + I_{c,b}(B_a)) \int_0^T v_2 \,\mathrm{d}t}, \tag{8}$$

where I_{2-} and $I_{c,b}(B_a)$ are the secondary current in the negative part of the ac waveform and bridge critical current under applied field, respectively. The resulting efficiency is then independent of voltage waveform.

$$\eta = \frac{i_L}{i_L + I_{c,b}(B_a) + I_{2-}}. \tag{9}$$

Assuming the two switches are identical, the negative waveform trough cannot exceed $I_{c,b}(B_a)$.

$$\eta = \frac{i_L}{i_L + 2I_{b,c}(B_a)} \tag{10}$$

The secondary must supply a positive waveform peak of $i_{2+} = i_L + i_b$ such that the bridge current exceeds I_c to produce voltage when switched. To prevent the load current being limited by the bridge during the current maintenance when the secondary current is negative, the switches must have a larger self-field critical current $I_{c,b}(0)$ than the combined load and bridge currents.

$$I_{c,b}(0) \geq i_L + I_{2-} = i_L + I_{c,b}(B_a) \tag{11}$$

Substituting (11) into (10) gives a limiting expression of only critical currents,

$$\eta \leq \frac{I_{c,b}(0) - I_{c,b}(B_a)}{I_{c,b}(0) + I_{c,b}(B_a)}. \tag{12}$$

This may be simplified by defining the depth of critical current modulation as a “switching factor” to represent the performance of the switching element

$$\kappa = \frac{I_{c,b}(0)}{I_{c,b}(B_a)}, \tag{13}$$

which gives efficiency as

$$\eta \leq \frac{\kappa - 1}{\kappa + 1}. \tag{14}$$

This analysis can be extended to the center-tap full-wave configuration (Fig. 1b)) by noting that similar limiting conditions on critical current 11 and flux conservation 1 apply.

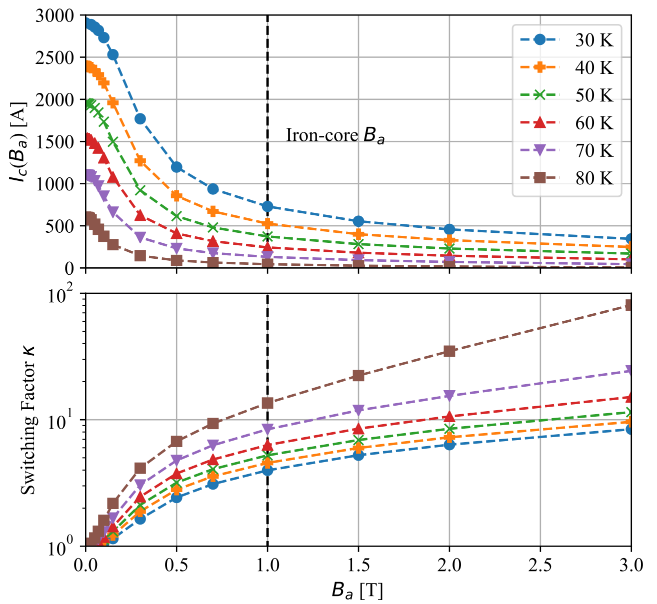

Fig. 2. Commercially characterized [29], [30] $I_{c,b}(B_a)$ response of SCN12700-210222-01 HTS tape and resulting switching factor κ at different temperatures. An iron-core B_a is shown as a black-dashed line.

The input waveform need only be asymmetric for a half-wave or passive rectifier; full-wave uses a symmetric (50% duty) square-wave of $\pm I_{c,b}(B_a)$ [10], which will reduce the requirements of the input transformer. The efficiency is still waveform independent.

In the period of a cycle, the power dissipated by switches in a centre-tap full-wave configuration is half that of a half-wave:

$$\eta = \frac{P_{\text{out}}}{P_{\text{out}} + \frac{1}{2}P_{\text{sw}}} = \frac{i_L}{i_L + I_{c,b}(B_a)} \tag{15}$$

$$\eta \leq \frac{I_{c,b}(0) - I_{c,b}(B_a)}{I_{c,b}(0)} = \frac{\kappa - 1}{\kappa} \tag{16}$$

Equations (14) and (16) for the ideal rectifier efficiency are both independent of voltage. Therefore, the voltage source and waveform are irrelevant in determining ideal rectifier efficiency. For a given current output capacity, the self-field critical current is fixed by (11) and the efficiency improves by suppression of critical current under applied field, defined as the switching factor κ.

From (13), κ, and therefore the ideal efficiency, of a rectifier is dependent only on the $J_c(B)$ properties of the superconducting tape used in the switch bridge. To interrogate the efficiency directly, the $J_c(B)$-characteristics of a candidate Gd-BCO tape, manufactured by SuNAM Co. Ltd., were measured. Characterization was performed commercially at the SuperCurrent Facility at Robinson Research Institute [29], [30] for a range of temperatures and applied fields B_a between 30 K and 80 K and up to 3 T, respectively. The results agree with manufacturer specifications and are shown in Fig. 2. The resulting switching factor κ was then calculated as the self-field (B_a = 0.0 T) I_c divided by $I_{c,b}(B_a)$. This was then used in (14) and (16) to produce the half- and full-wave ideal efficiencies.

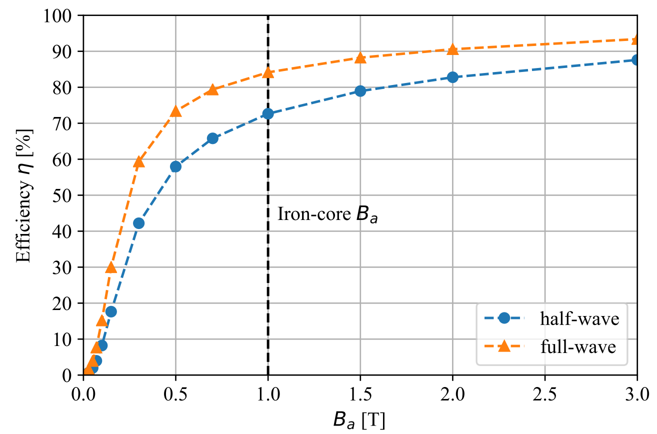

Fig. 3. Ideal Efficiency η of both half- (blue) and full-wave (orange) TRFP operating at 60 K using a range of applied fields B_a. Values were calculated from the 60 K $I_{c,b}(B_a)$ data in Fig 2.

Fig. 3 shows the ideal efficiency of both circuit topologies, which both increase at higher applied field due to the improvement in switching factor. Efficiency improves rapidly at lower applied fields, with diminishing returns as B_a increases due to the $J_c(B)$ response shown in Fig. 2. Switching also improves at higher temperature due to the poorer $J_c(B)$-characteristics of the tape close to critical temperature T_c=91 K. Thus, operating the flux pump at increased temperatures and applied fields is advantageous from an efficiency perspective. Indeed, this highlights the importance of the $J_c(B)$-characteristics of the tape in producing useful voltage [31].

The presented model is deliberately simplistic; neglecting ac loss, joint resistance, and circuit inductances to provide early tractability. Introducing these terms will be complicated, and beyond the scope of the present work. Ac loss terms relating to the changing applied field during switch actuation or the use of dynamic resistance switching will introduce magnetization loss. This will not significantly affect the power transfer efficiency during low frequency operation, but represents an additional heat loss term, preventing this model from accurately estimating the device's cryogenic losses. Joint resistances are unavoidable in HTS coated conductors and will limit the voltage output of the device, reducing efficiency. Inductances will introduce loss when currents change in the circuit, which may be significant in the charging loop.

III. Cryogenic Heat Load

The ideal efficiency model presented in Section II may be used to calculate the expected heat load of switching in the cryogenic environment. From (14) and (16), the switching loss can be calculated from a given power output P_{out} and efficiency.

$$P_{sw} = \dot{Q}_{cryo} = P_{\text{out}}\left(\frac{1}{\eta} - 1\right) \tag{17}$$

To calculate the cryogenic heat load of an ideal TRFP flux pump, one need only know the power output and efficiency, determined by switching factor κ.

TABLE I
DESIGN CONSTRAINTS OF REACTOR-LIKE* MAGNET COIL

Operational Current I_{coil}	60 kA
Inductance L	80 mH
Operational Temperature T_{coil}	20 K
Series Joint Resistance[a] R_j	100 nΩ
Charging Time t_{ch}	24 hours

*Compact tokamak with 18 TF magnets with total inductance of 1.5 H.
[a]Total resistance of HTS-HTS solder joint [32].

TABLE II
DESIGN PARAMETERS OF A 60 KA FLUX PUMP

Switch Temperature T_{sw}	60 K
Switch Applied Field B_a	1.0 T
Switching Factor κ	6.4
Full-wave Efficiency η	84%
Parallel Tapes n	45
Charging Voltage V_DC (avg./max.)	55/110 mV
Charging Power P_{ch} (avg./max.)	1650/3300 W
Heat Load $\dot{Q}_{ch}$ (η=84%)	314/728 W
qPCM Voltage V_{qPCM}	6 mV
qPCM Power P_{qPCM}	360 W
Heat Load $\dot{Q}_{qPCM}$ (η=84%)	69 W

IV. DESIGN PARAMETERS OF A 60 KA FLUX PUMP

Using the models presented in Sec. II and III, the design parameters of a 60 kA Flux Pump for a fusion TF coil can be determined in the setting of an reactor-like magnet, whose specifications are summarized in Table I. To prevent the output from being bridge limited, a cable of n tapes must be used in parallel, where n can be calculated with (11) using critical current data (such as in Sec. II). Decreasing the operational temperature increases critical current, reducing the number of parallel tapes needed. However, it also prevents effective critical current suppression due to applied field, reducing efficiency. An intermediate temperature of operation must be chosen to balance these competing effects. This could be achieved by locating the flux pump in a separate cryostat. In the proceeding example, an operational temperature of 60 K and 1.0 T of applied field, similar to that of an iron-core switching coil, are chosen. The resulting design parameters of a 60 kA flux pump are summarized in Table II.

The cryogenic heat load from switching can be calculated from the power output of the device using (17). During qPCM, the flux pump need only overcome the joint resistance, expected to be on the order of 100 nΩ, resulting in an output power of 360 W. During a 24-hour charging period, a maximum and average voltage of 110 mV and 55 mV, respectively, will be required. This results in average and maximum power outputs of 1.65 kW and 3.3 kW, respectively. Such voltage outputs are achievable with present switching capabilities [33]. The resulting cryogenic heat load of the flux pump during charging and qPCM are then 314 W and 69 W, respectively. This is a major reduction from the minimum ∼6 kW of heat load associated with current leads connecting room temperature supplies to a magnet coil at 4.5 K [6].

The overall size of the flux pump can also be estimated. The main components of the flux pump are the transformer and switches. The cross-sectional area to prevent the transformer from saturating is well understood, and can be calculated from

$$S_{iron} = \frac{V_{DC}}{B_{sat} f N_2} \tag{18}$$

where V_DC is the dc output voltage, N_2 is the number of turns of the superconducting secondary, β is the saturation field of the iron core, and f is the frequency of operation. This is larger than what is required by an ac sine wave input to allow for the derating of the transformer [34]. For a flux pump operating at 10 Hz with N_2=10, a core area of (35 mm)^2 will be enough to supply 110 mV. The room temperature copper windings will not contribute significantly to the size of the transformer.The transformer volume can be estimated to be only 7.5 dm^3. The switch can similarly be calculated to have a volume of 79 dm^3, or 0.16 m^3 for a pair. The total volume of the flux pump itself includes joints between these components and the load coil, but would likely be less than 0.2 m^3; small compared to present power electronics. Therefore, an reactor-like tokamak with 18 field coils would need a flux pump cryostat of only 3.6 m^3; comparable to a standard server rack. Additional space would be required for the transformer and switch coil power supplies, but would doubtless be much smaller than the 5 ha. of switching and bus bars implemented for the ITER project [4].

V. CONCLUSION

In this work, we have presented an ideal power transfer efficiency model for transformer-rectifier flux pumps. In this model, efficiency is determined only by the switch performance, represented by the switching factor defined as the ratio of self-field and applied field critical current of the switching element. The performance of the switch and subsequent efficiency is improved by increasing applied field and operating at temperatures with favourable $J_c(B)$-characteristics. Efficiencies of $> 80\%$ can be achieved in both the half- and full-wave circuit topologies.

The ideal efficiency model presented was used to calculate the expected heat load of a transformer-rectifier flux pump when charging and maintaining the coil current of an ITER-like TF magnet. It was found that for a full-wave flux pump operating at 60 K and 1.0 T of applied field, the expected heat load during charging and current maintenance is only 314 W and 69 W respectively. This is almost 10^2 less than the heat leak associated with current leads to room temperature, significantly reducing the required cooling power of the reactor. Such a flux pump solution would improve the overall power balance of a tokamak reactor. Flux pumping also enables the toroidal field to be sustained persistently, allowing for steady-state reactor designs using non-inductive heating and current drive methods [35], [36].

The presented model is simplistic to ensure initial tractability. It is expected that, realistically, transformer and switch coil losses, finite circuit inductance, joint resistance, and ac loss in the conductor will all contribute to the overall wall-plug efficiency of a transformer rectifier flux pump. It is also unclear how the plasma may couple to TF coils driven by the low voltage supplied by flux pumps [37]. Future work will need to address these issues.

References

[1] N. Mitchell, D. Bessette, R. Gallix, C. Jong, J. Knaster, P. Libeyre, C. Sborchia, and F. Simon, "The ITER magnet system," vol. 18, no. 2, pp. 435–440.

[2] H. W. Weijers, U. P. Trociewitz, W. D. Markiewicz, J. Jiang, D. Myers, E. E. Hellstrom, A. Xu, J. Jaroszynski, P. Noyes, Y. Viouchkov, and D. C. Larbalestier, "High field magnets with HTS conductors," vol. 20, no. 3, pp. 576–582.

[3] R. Aymar, P. Barabaschi, and Y. Shimomura, "The ITER design," vol. 44, no. 5, pp. 519–565. [Online]. Available: https://doi.org/10.1088/0741-3335/44/5/304

[4] J. Tao, I. Benfatto, J. K. Goff, A. Mankani, F. Milani, I. Song, H. Tan, and J. Thomsen, "ITER coil power supply and distribution system," in *2011 IEEE/NPSS 24th Symposium on Fusion Engineering*, pp. 1–8.

[5] A. Ballarino, P. Bauer, Y. Bi, A. Devred, K. Ding, A. Foussat, N. Mitchell, G. Shen, Y. Song, T. Taylor, Y. Yang, and T. Zhou, "Design of the HTS current leads for ITER," vol. 22, no. 3, pp. 4 800 304–4 800 304.

[6] A. Ballarino, "Current leads, links and buses," p. 12, #goals Â minimum conventional loss of 1.1 W/kA HTS leads are the same, plus the joint resistance between resistive and HTS Assuming similar joint resistance in the HTS FP set-up, the minimum heat inleak is a target for the in-cryo losses of the flux pump power supply. 1.1 W/kA 50 kW power supply can loose up to 55 W of in-cryo heat dissipation.

[7] V. Kalinin, E. Tada, F. Millet, and N. Shatil, "ITER cryogenic system," vol. 81, no. 23, pp. 2589–2595. [Online]. Available: https://www.sciencedirect.com/science/article/pii/S0920379606001906

[8] L. van de Klundert and H. ten Kate, "Fully superconducting rectifiers and fluxpumps part 1: Realized methods for pumping flux," vol. 21, no. 4, pp. 195–206. [Online]. Available: https://linkinghub.elsevier.com/retrieve/pii/0011227581901958

[9] L. J. M. van de Klundert and H. H. J. ten Kate, "On fully superconducting rectifiers and fluxpumps. a review. part 2: Commutation modes, characteristics and switches," vol. 21, no. 5, pp. 267–277. [Online]. Available: https://www.sciencedirect.com/science/article/pii/0011227581900023

[10] M. P. Oomen, M. Leghissa, G. Ries, N. Proelss, H. Neumueller, F. Steinmeyer, M. Vester, and F. Davies, "HTS flux pump for cryogen-free HTS magnets," vol. 15, no. 2, pp. 1465–1468.

[11] Z. Bai, G. Yan, C. Wu, S. Ding, and C. Chen, "A novel high temperature superconducting magnetic flux pump for MRI magnets," vol. 50, no. 10, pp. 688–692. [Online]. Available: http://www.sciencedirect.com/science/article/pii/S0011227510001438

[12] C. Hoffmann, D. Pooke, and A. D. Caplin, "Flux pump for HTS magnets," vol. 21, no. 3, pp. 1628–1631. [Online]. Available: http://ieeexplore.ieee.org/document/5675712/

[13] J. Geng and T. A. Coombs, "Mechanism of a high- T_c superconducting flux pump: Using alternating magnetic field to trigger flux flow," vol. 107, no. 14, p. 142601. [Online]. Available: http://aip.scitation.org/doi/10.1063/1.4932950

[14] ——, "An HTS flux pump operated by directly driving a superconductor into flux flow region in the *Eâ€“ J* curve," vol. 29, no. 9, p. 095004. [Online]. Available: https://iopscience.iop.org/article/10.1088/0953-2048/29/9/095004

[15] J. Ma, J. Geng, and T. A. Coombs, "Flux pumping for non-insulated and metal-insulated HTS coils," vol. 31, no. 1, p. 015018. [Online]. Available: https://doi.org/10.1088/1361-6668/aa99f2

[16] P. Zhou, G. Ma, Y. Deng, X. Nie, Y. Zhai, K. Liu, H. Zhang, and Y. Li, "A contactless self-regulating HTS flux pump," vol. 30, no. 4, pp. 1–6.

[17] T. A. Coombs, J. Geng, L. Fu, and K. Matsuda, "An overview of flux pumps for HTS coils," vol. 27, no. 4, pp. 1–6.

[18] R. Mataira, M. Ainslie, A. Pantoja, R. Badcock, and C. Bumby, "Mechanism of the high- t c superconducting dynamo: Models and experiment," vol. 14, no. 2, p. 024012, the Magnum Opus of HTS Dynamo physics Â Combines the previously reported model with a simple experiment to explain how precisely a dc current is produced from an ac dynamo source. [Online]. Available: https://link.aps.org/doi/10.1103/PhysRevApplied.14.024012

[19] K. Hamilton, A. E. Pantoja, J. G. Storey, Z. Jiang, R. A. Badcock, and C. W. Bumby, "Design and performance of a â€œsquirrel-cageâ€ dynamo-type HTS flux pump," vol. 28, no. 4, pp. 1–5. [Online]. Available: http://ieeexplore.ieee.org/document/8289321/

[20] J. Geng, T. Painter, P. Long, J. Gawith, J. Yang, J. Ma, Q. Dong, B. Shen, C. Li, and T. A. Coombs, "A kilo-ampere level HTS flux pump," vol. 32, no. 7, p. 074004. [Online]. Available: https://iopscience.iop.org/article/10.1088/1361-6668/ab1821

[21] J. Geng, C. W. Bumby, and R. A. Badcock, "Maximising the current output from a self-switching kA-class rectifier flux pump," vol. 33, no. 4, p. 045005. [Online]. Available: https://iopscience.iop.org/article/10.1088/1361-6668/ab6957

[22] S. Lee, W.-S. Kim, Y. Kim, J.-Y. Lee, S.-H. Park, J.-K. Lee, G.-W. Hong, S. Kim, J. Han, Y. J. Hwang, and K. Choi, "Persistent current mode operation of a 2g HTS coil with a flux pump," vol. 26, no. 4, pp. 1–4. [Online]. Available: http://ieeexplore.ieee.org/document/7397951/

[23] C. W. Bumby, A. E. Pantoja, H. Sung, Z. Jiang, R. Kulkarni, and R. A. Badcock, "Through-wall excitation of a magnet coil by an external-rotor HTS flux pump," vol. 26, no. 4, pp. 1–5.

[24] Z. Jiang, K. Hamilton, N. Amemiya, R. A. Badcock, and C. W. Bumby, "Dynamic resistance of a high-tc superconducting flux pump," vol. 105, no. 11, p. 112601. [Online]. Available: https://aip.scitation.org/doi/10.1063/1.4895732

[25] B. Leuw, J. Geng, J. H. P. Rice, D. Moseley, and R. A. Badcock, "Demonstration of a half-wave superconducting transformer-rectifier flux pump (strfp) using jc(b) switches," 2021, unpublished Manuscript.

[26] J. D. D. Gawith, J. Geng, C. Li, B. Shen, X. Zhang, J. Ma, and T. A. Coombs, "A half-bridge HTS transformerâ€“rectifier flux pump with two AC field-controlled switches," vol. 31, no. 8, p. 085002. [Online]. Available: https://doi.org/10.1088/1361-6668/aac86d

[27] C. Li, S. Wang, H. Jia, J. He, B. Li, and T. A. Coombs, "Impacts of the saturated transformer on the HTS flux pump," vol. 31, no. 8, pp. 1–4.

[28] K. Hamilton, R. Mataira, J. Geng, C. Bumby, D. Carnegie, and R. Badcock, "Practical estimation of HTS dynamo losses," vol. 30, no. 4, pp. 1–5.

[29] N. M. Strickland, C. Hoffmann, and S. C. Wimbush, "A 1 kA-class cryogen-free critical current characterization system for superconducting coated conductors," vol. 85, no. 11, p. 113907. [Online]. Available: http://aip.scitation.org/doi/10.1063/1.4902139

[30] S. C. Wimbush and N. M. Strickland, "A public database of high-temperature superconductor critical current data," vol. 27, no. 4, pp. 1–5.

[31] R. C. Mataira, M. D. Ainslie, R. A. Badcock, and C. W. Bumby, "Origin of the DC output voltage from a high-tc superconducting dynamo," vol. 114, no. 16, p. 162601. [Online]. Available: https://aip.scitation.org/doi/10.1063/1.5085226

[32] Y. Kim, J. BascuÃ±Ã¡n, T. Lecrevisse, S. Hahn, J. Voccio, D. K. Park, and Y. Iwasa, "YBCO and bi2223 coils for high field LTS/HTS NMR magnets: HTS-HTS joint resistivity," vol. 23, no. 3, pp. 6 800 704–6 800 704.

[33] C. Li, J. Geng, J. Gawith, B. Shen, X. Zhang, H. Zhang, J. Ma, and T. A. Coombs, "Design for a persistent current switch controlled by alternating current magnetic field," vol. 28, no. 4, pp. 1–5.

[34] C. P. Steinmetz, "On the law of hysteresis," vol. 9, pp. 3–64, reprinted under the title â€A Steinmemtz contribution to the ac power revolutionâ€, introduction by J. E. Brittain, in Proceedings of the IEEE 72(2) 1984, pp. 196-221. [Online]. Available: https://ia600708.us.archive.org/view_archive.php?archive=/22/items/crossref-pre-1909-scholarly-works/10.1109%252Fpaiee.1909.6660362.zip&file=10.1109%252Ft-aiee.1892.5570437.pdf

[35] Y. A. Podpaly, G. M. Olynyk, M. L. Garrett, P. T. Bonoli, and D. G. Whyte, "The lower hybrid current drive system for steady-state operation of the vulcan tokamak conceptual design," vol. 87, no. 3, pp. 215–223. [Online]. Available: https://www.sciencedirect.com/science/article/pii/S0920379611006314

[36] M. Austin, A. Marinoni, M. Walker, M. Brookman, J. deGrassie, A. Hyatt, G. McKee, C. Petty, T. Rhodes, S. Smith, C. Sung, K. Thome, and A. Turnbull, "Achievement of reactor-relevant performance in negative triangularity shape in the DIII-d tokamak," vol. 122, no. 11, p. 115001. [Online]. Available: https://link.aps.org/doi/10.1103/PhysRevLett.122.115001

[37] N. Mitchell, J. Zheng, C. Vorpahl, V. Corato, C. Sanabria, M. Segal, B. N. Sorbom, R. A. Slade, G. Brittles, R. Bateman, Y. Miyoshi, N. Banno, K. Saito, A. Kario, H. H. J. Ten Kate, P. Bruzzone, R. Wesche, T. Schild, N. Bykovskiy, A. Dudarev, M. G. Mentink, F. J. Mangiarotti, K. Sedlak, D. Evans, D. C. van der Laan, J. D. Weiss, M. Liao, and G. Liu, "Superconductors for fusion: a roadmap." [Online]. Available: http://iopscience.iop.org/article/10.1088/1361-6668/ac0992